Supporting Information

Influences of fullerenol on hIAPP aggregation: amyloid inhibition and mechanistic aspects

Cuiqin Bai,[a] Dongdong Lin, [a, b] Yuxiang Mo,[a, c] Jiangtao Lei,[a] Yunxiang Sun,[a] Luogang Xie, [a, d] Xinju Yang,[a] and Guanghong Wei[*, a]

[a] Department of Physics, State Key Laboratory of Surface physics, Key Laboratory for Computational Physical Science (Ministry of Education), Fudan University, Shanghai 200433, People's Republic of China

[b] Department of Microelectronic Science and Engineering Science Faculty of Science, Ningbo University, Ningbo 315211, P. R. China.

[c] College of Physical Science and Technology, Guangxi Normal University, 15 Yucai Road, Guilin, 541004, China.
[d] College of Physics and Information Engineering, Henan Normal University, Xinxiang 453007, People's Republic of China.

This material contains details of REMD simulation, convergence check of REMD simulations, experiment details and nine supplementary figures.

Construction of initial states

The initial conformation of a hIAPP1-37 monomer with helical structure was taken from protein data bank (PDB id: 2L86). By performing a MD simulation at a high temperature of 750 K, we obtained extended coil states of hIAPP, from which 24 coil conformations were randomly selected. Each two chains were placed in cross, parallel or antiparallel orientation with a minimum distance of 1.0 nm between the two hIAPP chains (Figure S1). We calculated the pKa of the sidechain of H18 in the 24 conformations using Poisson-Boltzmann electrostatics calculations[1]. The pKa value is 6.35±0.11, ranging from 6.21 to 6.60, which is smaller than the pH value of 7.3. Thus, the sidechain of H18 should be mostly neutral. The exchange between two adjacent replicas was attempted every 1000 integration steps and the average acceptance ratios for each system is ~15%. Bond length of peptides and water molecules were constrained, respectively, using the LINCS[2] and SETTLE[3] algorithms, allowing an integration time step of 2 fs. The van der Waals interactions were calculated using a cutoff of 1.4 nm.

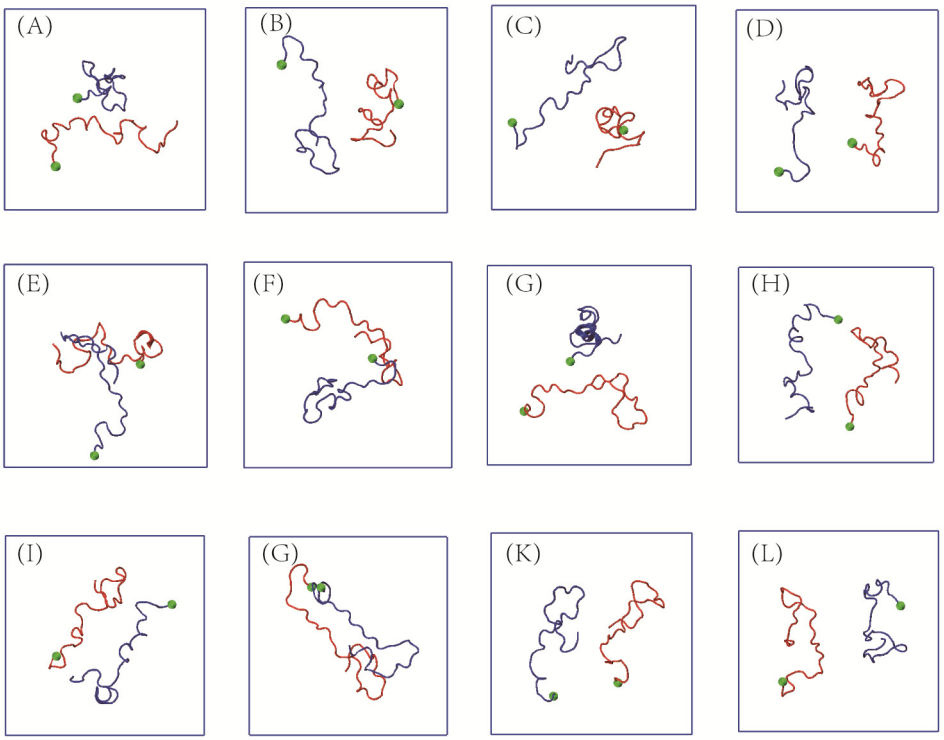

Figure S1. The initial states of hIAPP dimer used for our REMD simulations. Two hIAPP chains are colored in blue and red. The green balls refer to the C_α atoms of the N-terminal residues.

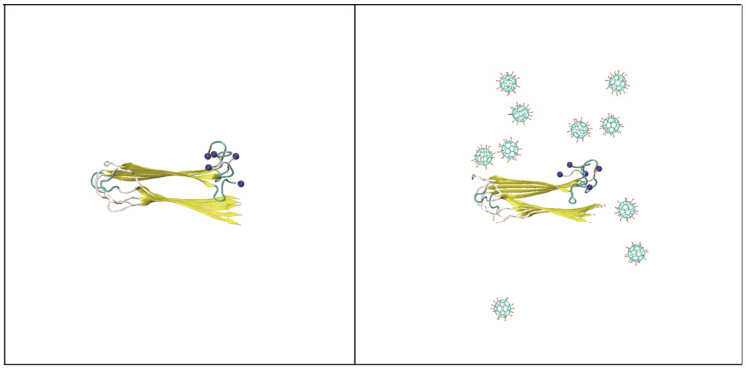

Figure S2. The initial conformations of (A) hIAPP-fibril, (B) hIAPP-fibril+C60$(OH)_{24}$. The blue balls refer to the C_α atoms of the N-terminal residues K1.

Temperature lists of REMD simulation for isolated hIAPP dimer and hIAPP dimer with nanoparticles

The temperature list is: 306.00, 307.96, 309.92, 311.90, 313.88, 315.88, 317.89, 319.89, 321.92, 323.95, 326.00, 328.06, 330.12, 332.20, 334.29, 336.38, 338.49, 340.61, 342.74, 344.88, 347.03, 349.19, 351.36, 353.54, 355.73, 357.94, 360.16, 362.38, 364.62, 366.87, 369.13, 371.40, 373.68, 375.97, 378.28, 380.60, 382.92, 385.25, 387.60, 389.96, 392.27, 394.66, 397.06, 399.47, 401.90, 404.33, 406.78, 409.24 K.

Convergence check of REMD simulations

We checked the convergence of the simulations by comparing each of the following four parameters of hIAPP dimer within two time intervals (200-280 ns & 280-360 ns) at 310 K, including the probability density functions (PDF) of the H-bonds (Figure S3) and Rg (Figure S4), the average probability of each secondary structure (Figure S5), residue-based secondary structure propensity (Figure S6).

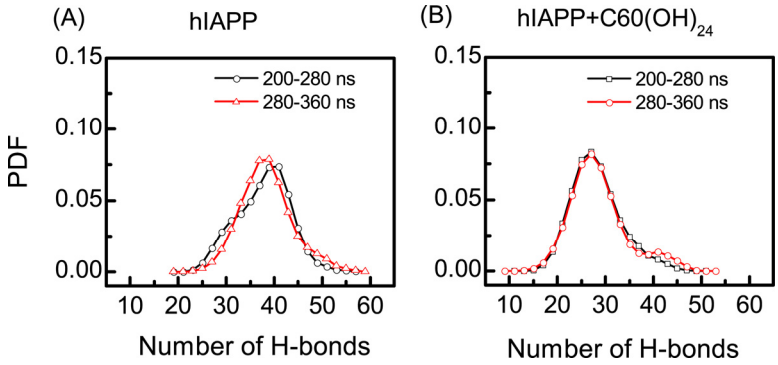

Figure S3. Probability density function (PDF) of the number of hydrogen bonds (H-bonds) of hIAPP dimer in the three different system: (A) hIAPP; (B) hIAPP+C60(OH)$_{24}$ within two different time intervals.

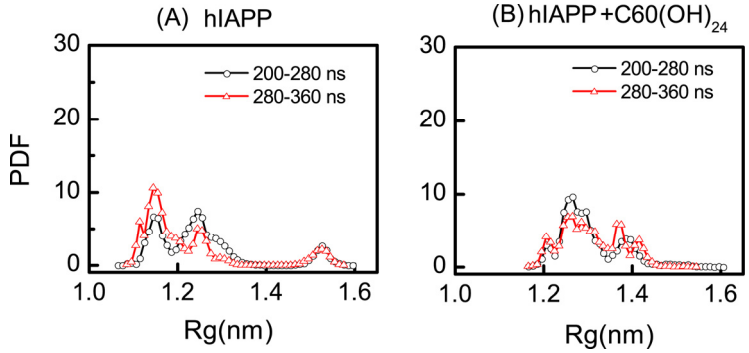

Figure S4. Probability density function (PDF) of radius of gyration (Rg) of hIAPP dimer in the three different systems: (A) hIAPP; (B) hIAPP+C60(OH)$_{24}$ within two different time intervals.

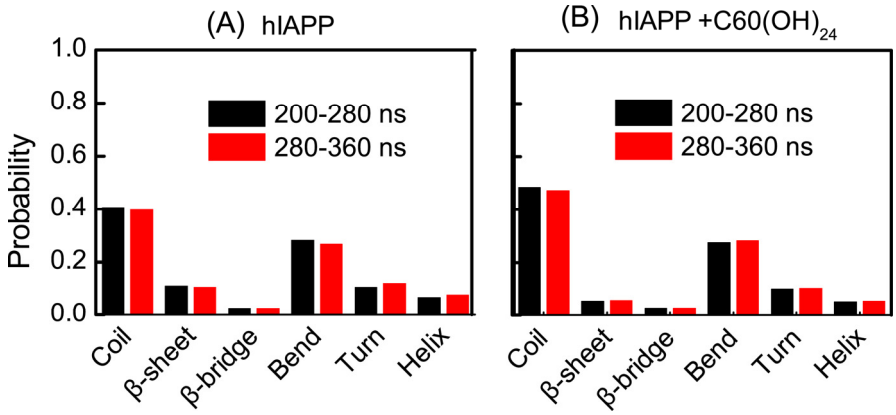

Figure S5. The probability of each secondary structure averaged over all residues of hIAPP dimer in hIAPP (A) and hIAPP+C60(OH)$_{24}$ (B) systems, using two different time intervals.

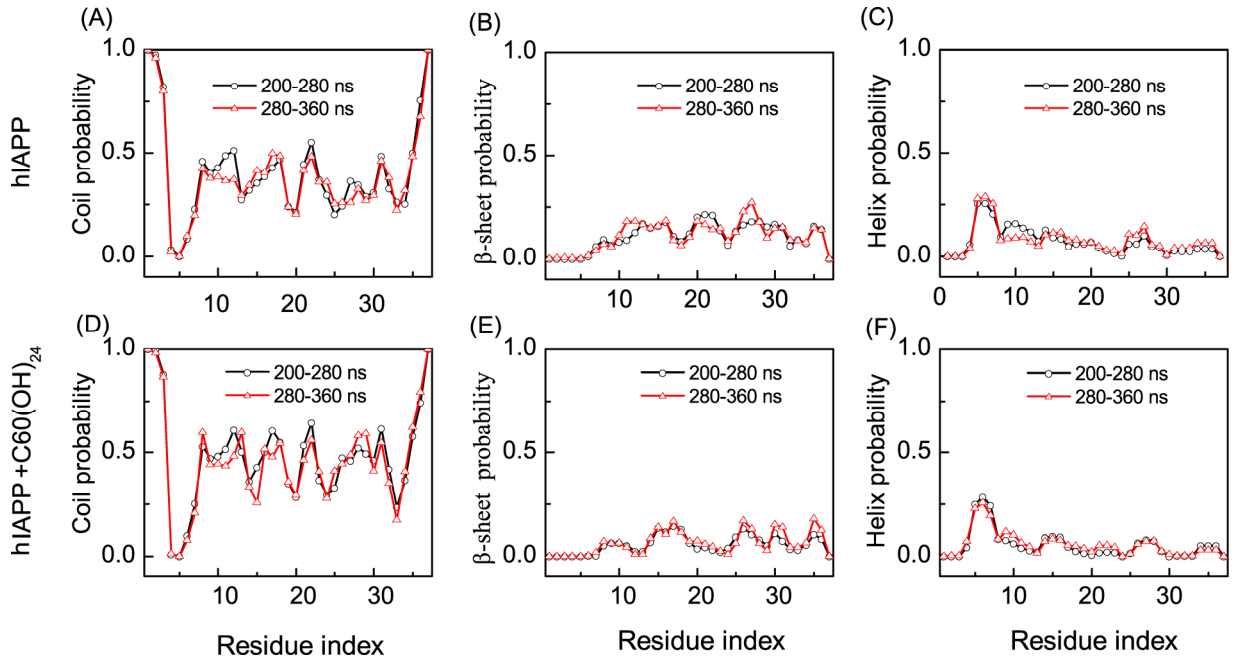

Figure S6. Secondary structure propensity as a function of amino acid residue within two time intervals for the hIAPP (A, B and C) and hIAPP+C60(OH)$_{24}$ (D, E and F).

Experiment sample preparation and experiment method

AFM and EFM measurements. In the first pass, AFM topography was measured in the conventional tapping mode. In the second pass, the AFM tip was lifted to the pre-set height so that the influence of van der Waals force can be excluded. Then, the phase shift signal related to the electrical force gradient was measured by applying a DC bias between the Pt coated Si tip and the sample. As EFM tip only senses with long range electrostatic forces without entering the repulsive contact regime, the influence of topography factor on the phase shift was excluded by lifting enough height (20 nm). When in measurements, a bias of -5 V was input on the sample.

ThT Fluorescence measurements. The measured samples were prepared by mixing 200 μL hIAPP solution with 10 μL ThT (1 mM) and 790 μL PBS solutions in a quartz cell. For comparison, the ThT control sample was prepared by mixing 10 μL ThT (1 mM) solution with 990 μL PBS solution. The mean and standard error (SE) were obtained by repeating three times in each sample.

Cell Viability. SH-SY5Y cells were incubated in the dulbecco's modified eagle medium (DMEM) medium with 10% calf serum, 100 units/mL penicillin, 100 μg/mL neomycin, and 100 μg streptomycin in a humidified standard incubator at 37℃, with a 5% CO_2 atmosphere. The cells were washed with PBS solution three times to remove the unassociated compounds and replenish with fresh medium. When the cells reached 80% confluence, 10 μL solutions of hIAPP and hIAPP+fullerenol were separately added into wells and incubated with medium for 3 h. The final concentration is about 1 μM for hIAPP and 2 μM for fullerenol. Then a 10 μL WST-1 solution (5 mg/mL) was added into each well for incubation of another 2 h.

EFM measurements were carried out to investigate the coexistence of hIAPP with fullerenols. The sample of pure hIAPP display clearer phase shift than that of hIAPP+fullerenols (Figure S7). The maximum phase shift of pure hIAPP reaches 1200 (4 day) millidegrees, while that of hIAPP+ fullerenols dramatically decrease to 200 millidegrees. The decrease of phase shift is mainly attributed to the low dielectric permittivity of hIAPP+fullerenols hybrid compound compared to pure hIAPP aggregates[4]. Consequently, EFM gives direct evidence that the large aggregates are composed of hIAPP and fullerenols.

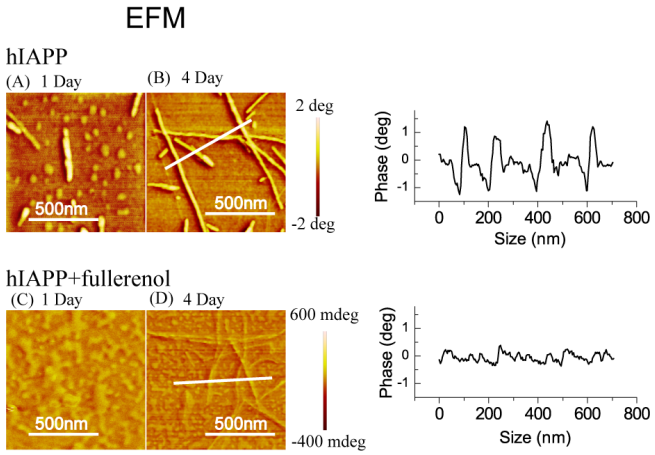

Figure S7. EFM phase images of hIAPP aggregates with/without fullerenols at different co-incubation time.

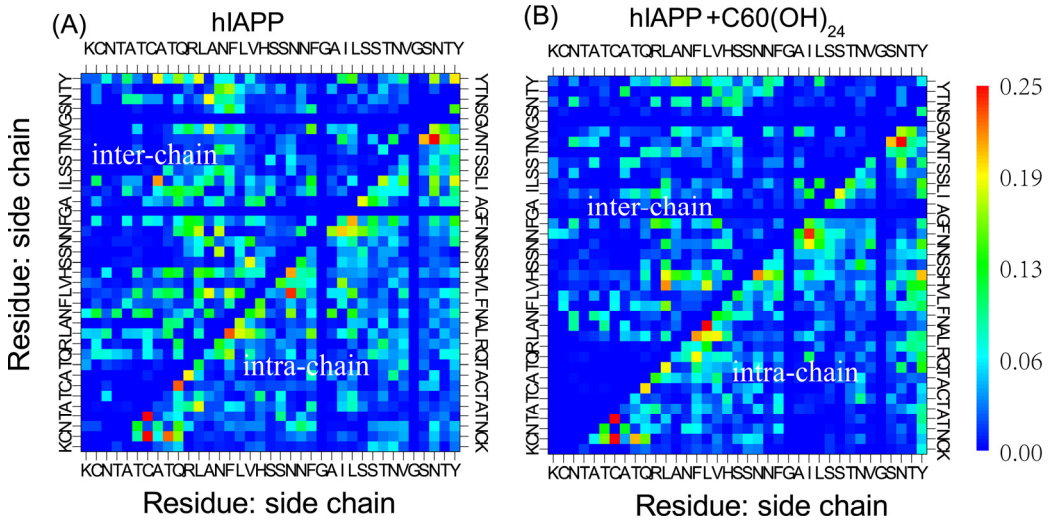

Figure S8. Inter- and intra-chain pairwise residue SC-SC contact probability maps for isolated hIAPP dimer (A) and hIAPP dimer in the presence of $C60(OH)_{24}$ (B).

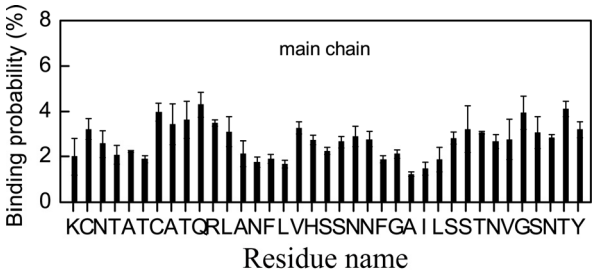

Figure S9. Binding probabilities of $C60(OH)_{24}$ with main chain atoms of each residue of hIAPP in hIAPP+$C60(OH)_{24}$ systems.

Reference

1. T. J. Dolinsky, J. E. Nielsen, J. A. McCammon and N. A. Baker, *Nucleic Acids Res*, 2004, **32**, W665-W667.
2. B. Hess, H. Bekker, H. J. C. Berendsen and J. G. E. M. Fraaije, *J Comput Chem*, 1997, **18**, 1463-1472.
3. S. Miyamoto and P. A. Kollman, *J Comput Chem*, 1992, **13**, 952-962.
4. M. H. Zhao, X. H. Gu, S. E. Lowther, C. Park, Y. C. Jean and T. Nguyen, *Nanotechnology*, 2010, **21**.